Development 125, 813-824 (1998)
Printed in Great Britain © The Company of Biologists Limited 1998
DEV9583

Cranial and cardiac neural crest defects in endothelin-A receptor-deficient mice

David E. Clouthier[1,2], Kiminori Hosoda[1,2,‡], James A. Richardson[3], S. Clay Williams[1,2], Hiromi Yanagisawa[4], Tomoyuki Kuwaki[5,*], Mamoru Kumada[5,†], Robert E. Hammer[1,4] and Masashi Yanagisawa[1,2,§]

[1]Howard Hughes Medical Institute, [2]Departments of Molecular Genetics, [3]Pathology and [4]Biochemistry, University of Texas Southwestern Medical Center at Dallas, 5323 Harry Hines Boulevard, Dallas, Texas 75235, USA
[5]Department of Physiology, Faculty of Medicine, University of Tokyo, Tokyo 113, Japan

*Present address: Department of Physiology, Chiba University School of Medicine, Chiba 260, Japan
†Present address: St Luke's College of Nursing, Tokyo 104, Japan
‡Present address: Second Department of Internal Medicine, Faculty of Medicine, Kyoto University, Kyoto 606, Japan
§Author for correspondence (e-mail: afcsushi@aol.com)

Accepted 8 December 1997: published on WWW 4 February 1998

SUMMARY

Neural crest cells arise in the dorsal aspect of the neural tube and migrate extensively to differentiate into a variety of neural and non-neural tissues. While interactions between neural crest cells and their local environments are required for the proper development of these tissues, little information is available about the molecular nature of the cell-cell interactions in cephalic neural crest development. Here we demonstrate that mice deficient for one type of endothelin receptor, ET_A, mimic the human conditions collectively termed CATCH 22 or velocardiofacial syndrome, which include severe craniofacial deformities and defects in the cardiovascular outflow tract. We show that ET_A receptor mRNA is expressed by the neural crest-derived ectomesenchymal cells of pharyngeal arches and cardiac outflow tissues, whereas ET-1 ligand mRNA is expressed by arch epithelium, paraxial mesoderm-derived arch core and the arch vessel endothelium. This suggests that paracrine interaction between neural crest-derived cells and both ectoderm and mesoderm is essential in forming the skeleton and connective tissue of the head. Further, we find that pharyngeal arch expression of *goosecoid* is absent in ET_A receptor-deficient mice, placing the transcription factor as one of the possible downstream signals triggered by activation of the ET_A receptor. These observations define a novel genetic pathway for inductive communication between cephalic neural crest cells and their environmental counterparts.

Key words: Mouse, Craniofacial development, Heart development, G protein-coupled receptor

INTRODUCTION

Neural crest cells are a migratory population of cells that originate at the dorsal lip of the neural fold (Le Douarin et al., 1993; Bronner-Fraser, 1995). Once at their final destinations, they differentiate into a wide variety of derivatives, including epidermal melanocytes, neurons, endocrine and paraendocrine derivatives, and much of the bone, cartilage and connective tissue of the head and neck (Le Douarin, 1982; Noden, 1988). Migration, proliferation and differentiation of these cells are highly influenced by local environmental factors encountered during and after migration (Jessel and Melton, 1992; Le Douarin et al., 1993; Shah et al., 1996).

Crest cells that participate in craniofacial morphogenesis arise from the cephalic neural crest. Head development begins with cephalic neural crest cell migration from the posterior midbrain-hindbrain region into the pharyngeal arches in an axial level-specific pattern (Lumsden et al., 1991; Serbedzija et al., 1992; Kontges and Lumsden, 1996). Once there, the crest-derived ectomesenchyme undergoes inductive changes, resulting in the development of craniofacial bones and cartilages (Le Lievre and Le Douarin, 1975; Couly et al., 1993; Kontges and Lumsden, 1996). Interestingly, long-term fate mapping of cephalic neural crest cells has clearly shown a constrained pattern of cranial skeletomuscular connectivity with respect to the positional origin of the constitutive crest cells (Kontges and Lumsden, 1996). This may result from interaction of ectomesenchymal cells with paraxial mesoderm-derived cells that are segregated in the mesenchymal core of the arch (Trainor et al., 1994; Trainor and Tam, 1995), the anlage to the bulk of the musculature of the head and jaw. These two precursor cell types likely instruct each other to initiate the correct morphogenetic program. Development of neural crest cells within the pharyngeal arches relies upon the action of numerous transcription factors (Anderson, 1997). These factors guide migrating neural crest cells and later play a role in lineage determination, expansion and differentiation of neural crest derivatives. The first family of genes known to be involved in pharyngeal arch development were the *Hox* genes (Hunt et

al., 1991). Specific *Hox* genes are expressed in arches 2-6, leading to the idea that a 'Hox code' was responsible for the development of all but the first (mandibular) arch, which developed by default programming. However, recent targeted mutations of transcription factors in mice have now shown that many genes are involved in the development of not only the first, but all of the pharyngeal arches. Mice with *AP-2* (Schorle et al., 1996; Zhang et al., 1996), *Cart1* (Zhao et al., 1996), *Dlx-1* (Qiu et al., 1997), *Dlx-2* (Qui et al., 1995; Qiu et al., 1997), *goosecoid* (Rivera-Perez et al., 1995; Yamada et al., 1995), *MHox* (Martin et al., 1995), *Msx1* (Satokata and Maas, 1994), and *Otx2* (Matsuo et al., 1995) null mutations, as well as *RARαγ* double knockouts (Lohnes et al., 1994), all suffer defects in cephalic neural crest-derived skeletal elements. These mutations often produce overlapping phenotypes, suggesting that multiple factors form a combinatorial code to pattern individual skeletal elements. However, evidence of an actual signaling pathway, including upstream intercellular activators, has not yet been found.

Patterning of specific regions of the developing heart also depends on a subset of cephalic neural crest cells, termed the cardiac neural crest (Kuratani and Kirby, 1991; Kirby, 1993; Kirby and Waldo, 1995). Cardiac neural crest ablation experiments illustrate that the development of aortic arch arteries and the conotruncal region of the heart rely upon contribution from crest cells. Mouse genes whose null mutations affect the cardiac neural crest and disrupt these structures include *ActRIIB* (Oh and Li, 1997), *dHAND* (Srivastava et al., 1997), *HoxA3* (Chisaka and Capecchi, 1991), *NF-1* (Brannan et al., 1994), *NT-3* (Donovan et al., 1996) and *Pax3* (Conway et al., 1997). *RAR α1β2, αβ2, α1γα2, αγ* double mutants also exhibit related abnormalities (Mendelsohn et al., 1994). However, as in the cephalic neural crest, a distinct signaling pathway that might initiate an inductive developmental program has not been delineated.

One group of genes that may play a potential role in neural crest determination are the endothelins and their receptors. The endothelin (ET) pathway consists of three closely related small peptide ligands (ET-1, -2 and -3) that bind to one or both of the G protein-coupled endothelin receptors, ET_A and ET_B (Arai et al., 1990; Sakurai et al., 1990; Yanagisawa, 1994). Recent evidence shows that endothelins and their receptors are required for development of specific subsets of neural crest-derived tissues: e.g. the disruption of the ET-1 gene causes malformations in pharyngeal arch-derived structures and the heart (Kurihara et al., 1994), while mice deficient in either ET-3 or ET_B develop white spotted coats and aganglionic megacolon due to the absence of neural crest-derived melanocytes and enteric neurons (Baynash et al., 1994; Hosoda et al., 1994). The phenotype observed in *ET-3*/ET_B deficient mice does not overlap with that of *ET-1* deficient animals, indicating that the developmental effect of *ET-1* is not mediated by the ET_B receptor.

To define the developmental role of the ET_A receptor, we generated ET_A-null mice by gene targeting. $ET_A^{-/-}$ mice are born alive but suffer severe craniofacial and cardiovascular defects, similar to those observed in *ET-1* deficient mice, and die soon after birth. Examination of expression patterns of ET_A and *ET-1* during development suggests that ET-1/ET_A interaction defines a novel signaling pathway crucial for pharyngeal arch development. This pathway includes *goosecoid*, whose expression in the pharyngeal arches depends on ET_A signaling.

MATERIALS AND METHODS

Gene targeting

The targeting construct was designed to replace exons 5 and 6 of the ET_A gene, which corresponds to the sixth and seventh transmembrane domains of this G protein-coupled receptor. Homologous sequences for the ET_A gene were obtained from an EMBL3 mouse genomic library (Clonetech), and were composed of a 12-kb *Sal*I/*Sal*I fragment 5′ to exons 5 and 6 and a 1.2-kb *Sac*I/*Spe*I fragment 3′ to exons 5 and 6. A universal *neo-TK* template plasmid vector (Hosoda et al., 1994), which contains a neomycin gene cassette driven by the RNA polymerase II promoter as well as two tandem herpes simplex virus thymidine kinase cassettes, was used to construct the targeting vector. The targeting construct was electroporated into JH-1 ES cells (Hosoda et al., 1994) maintained on SNL76/7 fibroblast feeder layers (a gift from A. Bradley). Following selection with G418 and FIAU, surviving colonies were screened with three probes (see Fig. 1) to confirm homologous recombination by Southern blot analysis. Probes A and C were used following digestion of genomic DNA with *Xba*I, while probe B was used following digestion with *EcoR*I. Correctly targeted ES cell clones were injected into blastocysts from C57BL/6 mice to obtain chimeras, which transmitted the targeted allele in their germline. Genotypes of mice were confirmed using probe C. To establish the deletion on an inbred background, mice were bred with 129SvEv mice. Subsequent genotyping was performed by the polymerase chain reaction (PCR) using genomic DNA isolated from tail biopsies. Primers used to detect the mutant allele were 5′-TCGCCTTCTTGACGAGTTCTTCTGAG-3′ (neo) and 5′-TGGGAATGGACCTGAGTCCTCTGC-3′ (3′ to the neo cassette). Primers used to detect the wild-type allele were 5′-TCTGGTCAGTTCCTGCTTTCCTCCTGG-3′ (5′ to exon 5) and 5′-CGATGTAATCCATTAGCAGCAAGAAGCTGG-3′ (exon 6). The sizes of the amplified products for the mutant and wild-type alleles were 450 bp and 800 bp, respectively.

Radioligand binding assay

Skin from $ET_A^{+/-}$ and $ET_A^{-/-}$ E18.5 embryos were minced and seeded onto the bottom of a 25 cm^2 flask in Dulbecco's modified Eagle's medium (DMEM) plus 20% fetal calf serum. Outgrowths of mesenchymal cells were passaged every 3 days and passage five cells were used in the assay. The binding assay was performed as previously described (Sakurai et al., 1990), using ^{125}I-ET-1 (2,000 Ci/mmol; Amersham) as the tracer. Unlabled ET-1 (American Peptide), FR139317 (Fujisawa Pharmaceutical), an ET_A antagonist, or IRL1620 (American Peptide), an ET_B agonist, were used as competitors. Non-specific binding was determined in the presence of 1×10^{-7} unlabeled ET-1. The ratios of non-specific to specific binding in the absence of competitors were approximately 2% and 16% in the cell lines from the heterozygous and homozygous animals, respectively.

Respiratory responses

E18.5 embryos were delivered by Caesarean section and immediately tracheostomized with a polyethylene tube (SP8, Natsume, Tokyo) as previously described (Kuwaki et al., 1996). Mice were then placed in a warmed chamber (32-35°C) for at least 30 minutes before ventilation was measured. Mice were placed in a plastic chamber, where they initially breathed room air. They were then exposed to hypoxic (1:1 room air:N_2) or hypercapnic (5% CO_2–95% O_2) gas mixtures. During this time, P_{CO_2} and P_{O_2} in the chamber were continuously monitored (Respina IH26, San-Ei-Instruments). When the gas within the chamber reached equilibrium, ventilatory measurements were performed for 3-

5 minutes. Pressure within the chamber was measured with a transducer (Model TP603T, Nihon Kohden), amplified (Model AR601G, Nihon Kohden) and stored in a data recorder (Model XR-7000L, TEAC). After analog to digital conversion (MP100, Biopac Systems), the data was fed into a Macintosh computer for computation as previously described (Kuwaki et al., 1996).

Histology and in situ hybridizations

For routine analysis, embryos were fixed in Bouin's fixative, embedded and sectioned at 4 μm. Paraffin sections of embryos were stained with hematoxylin and eosin as previously described (Hosoda et al., 1994). For skeleton analysis, E18.5 embryos were collected, prepared and stained with alizarin red and alcian blue to examine bone and cartilage formation, respectively (Kochhar, 1973). Cartilaginous fetal skeletons (E12.5-E14.5) were prepared and stained with alcian blue (Jegalian and De Robertis, 1992). For in situ hybridizations, embryos were collected and fixed in 4% paraformaldehyde. Sectional in situ hybridizations were performed as described previously (Benjamin et al., 1997) except that riboprobes were labeled with both ^{35}S-CTP and ^{35}S-UTP (Amersham) using the Maxiscript In Vitro Translation Kit (Ambion). The *ET_A* probe was a 350 bp *Bam*HI-*Eco*RI fragment and the *ET-1* probe was a 380 bp *Sac*I-*Hin*dIII fragment, both from mouse cDNAs. Whole-mount in situ hybridizations were performed using E10.5 embryos as previously described (Wilkinson, 1992) using digoxigenin-labeled probes for *Dlx-1* (McGuinness et al., 1996) and *goosecoid* (Shawlot and Behringer, 1995). Embryos were genotyped by PCR using genomic DNA isolated from yolk sac.

Whole-mount immunohistochemistry

The immunohistochemistry protocol used was adapted from that of Davis et al., (1991). E10.5 and E11.5 embryos were collected and fixed in 4% paraformaldehyde at 4°C overnight. After rinsing in PBS, they were dehydrated through a graded series of methanols, bleached in 5% hydrogen peroxide in methanol for 5 hours and rinsed in 100% methanol. After rehydrating into PBS, embryos were blocked for 1 hour in 0.5% Triton X-100 and 2% skimmed milk powder in PBS (PBSMT) and then incubated overnight at 4°C with an anti-NF160 antibody (Sigma, #N5264) at a dilution of 1:100 in PBSMT. After rinsing 5 times for 1 hour each in PBSMT, embryos were incubated overnight at 4°C with a horseradish peroxidase-conjugated goat anti-mouse IgG antibody (Sigma, #A3682) at a dilution of 1:200 in PBSMT. After rinsing 5 times for 1 hour each in PBSMT, embryos were rinsed in 0.5% Triton X-100 and 2% BSA (PBT) for 5 minutes and then incubated with diaminobenzadine (DAB) using the Liquid DAB Substrate Kit (Zymed) and following the manufacturer's instructions. After rinsing in PBT twice for 10 minutes each, embryos were dehydrated through a graded methanol series and cleared in 2:1 benzyl benzoate:benzyl alcohol.

RESULTS

Developmental patterns of *ET_A* and *ET-1* expression in pharyngeal arches

Targeted disruption of the *ET-1* gene in mice results in craniofacial and cardiovascular defects (Kurihara et al., 1994) that are not observed in *$ET_B^{-/-}$* mice (Hosoda et al., 1994). These defects are therefore probably not a result of loss of ET_B signaling. The present study was designed to examine the role of the other known endothelin receptor, the ET_A receptor, in development of these tissues. In situ hybridization analysis found that cephalic crest cells become ET_A-positive as soon as they leave the rhombomeres, while the neural tube itself does not express ET_A (data not shown). At E9.5, *ET_A* mRNA was observed in migrating cephalic neural crest cells extending from the hindbrain into the pharyngeal arches (Fig. 1A). Message was also present in the facio-acoustic neural crest complex (Fig. 1A). The mesenchyme of pharyngeal

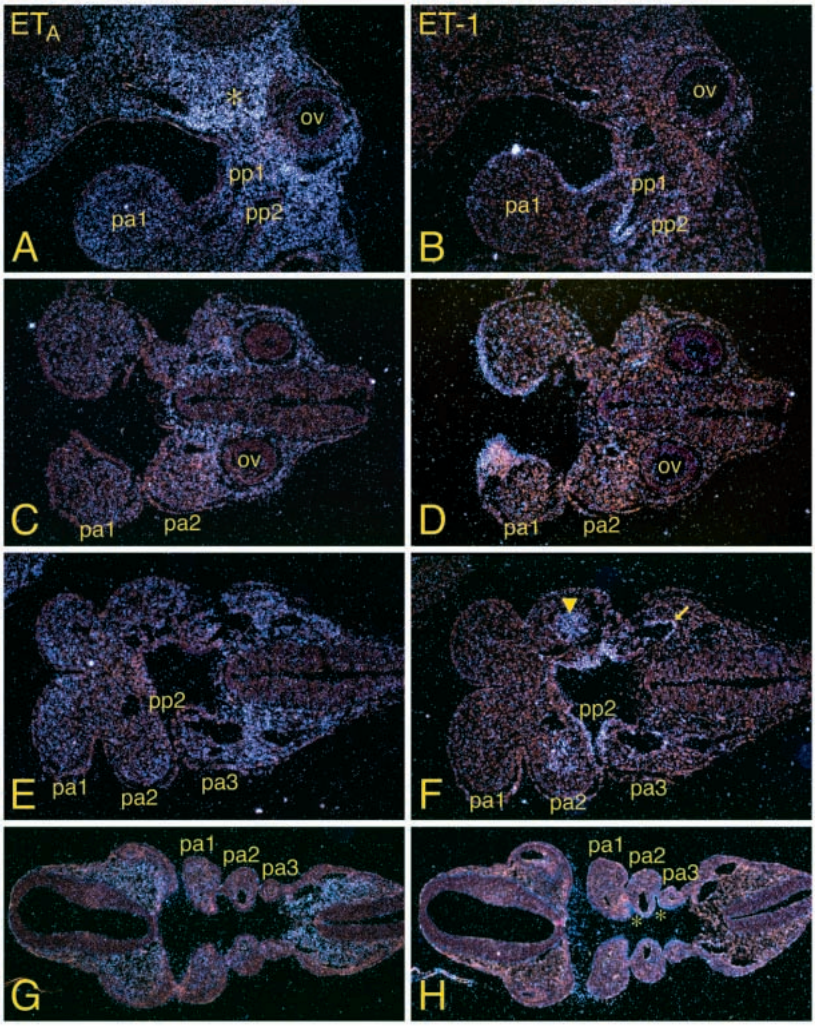

Fig. 1. In situ hybridization analysis of *ET_A* (A, C, E, G) and *ET-1* (B, D, F, H) transcripts in the pharyngeal arch region of E9.5 wild-type embryos. (A, B) Sections through the sagittal plane. *ET_A* mRNA is detected in head and first pharyngeal arch (pa1) mesenchyme, as well as in the facio-acoustic neural crest complex (*). *ET-1* mRNA is restricted to the epithelium of the arch and the endoderm of pharyngeal pouches (pp) 1 and 2. (C-F) Sections through the transverse plane. (C, E) *ET_A* mRNA is observed in the mesenchyme of the head and pharyngeal arches 1, 2 and 3. (D) *ET-1* mRNA is found on the arch epithelium. (F) *ET-1* mRNA is found in the endothelium of the communication between pharyngeal arch artery 3 and the dorsal aorta (arrow), and in the paraxial mesoderm core of arch 2 (arrowhead). (G, H) Sections through the frontal plane. The asterisks in (H) mark *ET-1* message in the pharyngeal pouches. ov, otic vesicle.

arches 1, 2 and 3 were also ET_A-positive, although the arch epithelium was negative (Fig. 1A,C,E,G). It is noteworthy that in Fig. 1E, ET_A message is less abundant in the core of arch 2. ET_A mRNA was also observed in head and body mesenchyme (Fig. 1A,C,E,G).

Conversely, *ET-1* message was confined to the ectodermal epithelium of arches 1, 2 and 3 and their associated endodermal pouch epithelia (Fig. 1B,D,F). Interestingly, *ET-1* mRNA was also observed in the paraxial mesoderm-derived core of arches 1 (data not shown) and 2 (Fig. 1F). Expression of *ET-1* in paraxial mesoderm, which gives rise to most of the muscles and vasculature of the head, has been documented before, but was interpreted as being simply arch mesenchyme staining (Maemura et al., 1996). As mentioned above, paraxial mesoderm does not mix with neural crest cells in the pharyngeal arches, but rather colonizes only the core mesenchyme (Trainor and Tam, 1995). Since neural crest cells overlay the mesoderm, it is likely that ET-1 in the mesoderm, together with ET-1 in the arch epithelium, acts on the ectomesenchymal cells to help further control craniofacial morphogenesis.

Expression of ET_A and *ET-1* in the developing heart

In situ hybridization analysis of the heart in E8.5 (data not shown) and E9.5 (Fig. 7E) wild-type embryos found abundant ET_A mRNA in the myocardium of the ventricle, atrium and bulbus cordis, as well as in the mesenchyme of the aortic arches. Conversely, *ET-1* expression was observed in the endocardium of the heart chambers and the endothelial lining of the arch arteries (Fig. 7F). This suggests that local interactions between cardiac neural crest-derived mesenchyme and the underlying endothelium of the arches results in initiation or continuation of a cardiac developmental program (see below).

Targeted disruption of the ET_A gene

To disrupt the ET_A gene, we constructed a targeting vector that would replace exons 5 and 6, which encode the sixth and seventh transmembrane domains, with a *neomycin* resistance cassette by homologous recombination. Two thymidine kinase (TK) genes were included in tandem at the 3′ end of the targeting vector as a negative selection marker for non-homologous recombination events (Fig. 2A). The targeting construct was electroporated into ES cells, and following selection for homologous recombination, surviving clones were screened by Southern blot (Fig. 2B). Correctly targeted clones were used to generate chimeric mice by blastocyst injection as described in Materials and Methods. Germline

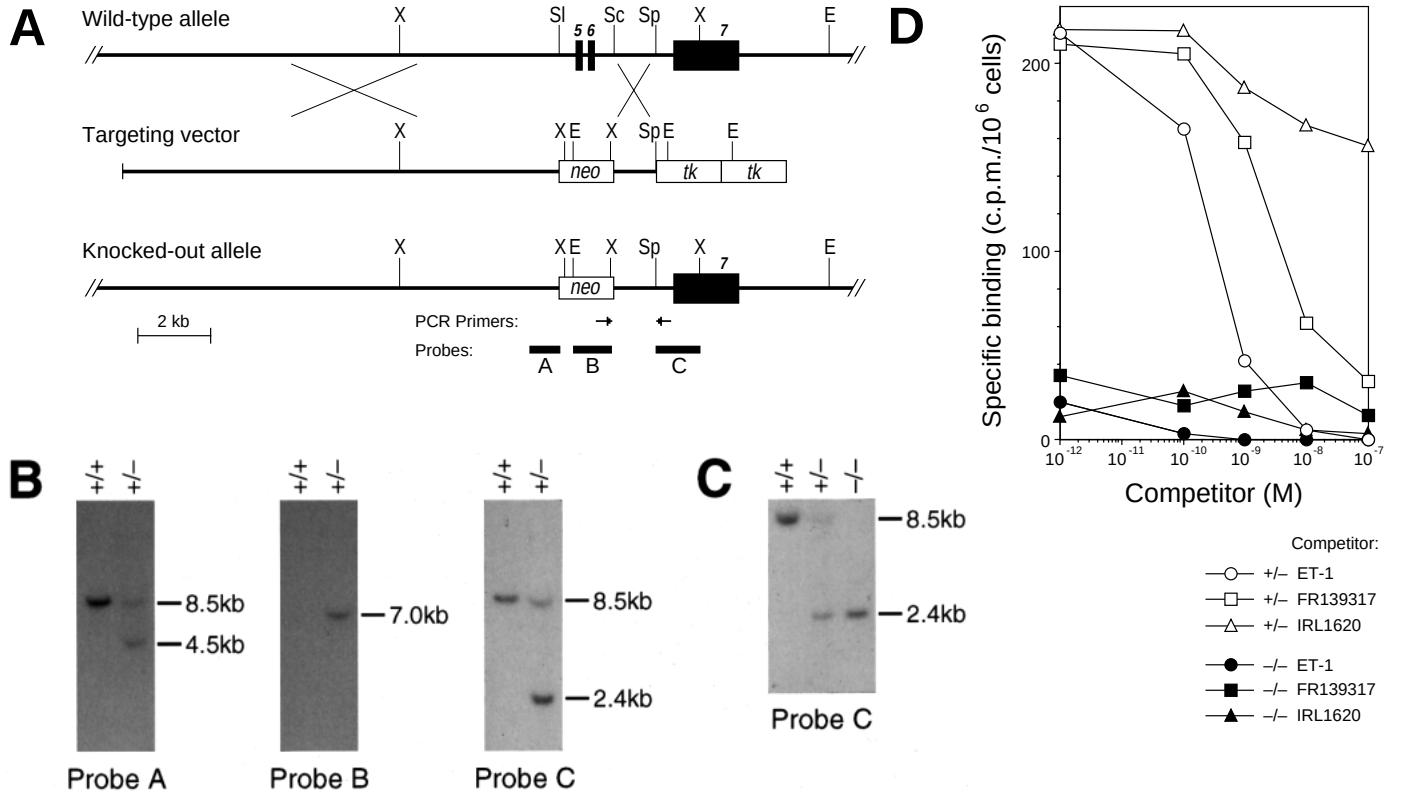

Fig. 2. Disruption of the ET_A gene. (A) Strategy for disruption of the ET_A gene. A partial map of the wild-type mouse ET_A gene, including exons 5 and 6, which encode the sixth and seventh transmembrane domains, respectively, is shown. Southern blot probes and PCR primers used are shown below the map of the targeted allele. Restriction enzymes: E, *Eco*RI; Sc, *Sac*I; Sl, *Sal*I; Sp, *Spe*I; X, *Xba*I. (B) Southern blot analysis of DNA from wild-type and ET_A mutant ES cells. Genomic DNA was digested with *Xba*I and the blot hybridized with the 5′ probe (probe A), the internal probe (probe B) or the 3′ probe (probe C). Wild-type (8.5 kb) and targeted (2.4, 4.5 or 7.0 kb) fragments are indicated. (C) Southern blot analysis of tail DNA from wild-type (+/+), heterozygous (+/–) and homozygous (–/–) mutant mice. The DNA was digested with *Xba*I and the blot hybridized with probe C. (D) Radioligand binding assay for the ET_A receptor protein. Unlabeled ET-1, FR139317 (an ET_A antagonist) or IRL1620 (an ET_B agonist) were used as competitors. Open and closed symbols indicate $ET_A^{+/-}$ and $ET_A^{-/-}$ cells, respectively.

transmission of the disrupted allele resulted in heterozygous mice that were healthy and fertile. The number of homozygous mutant mice obtained from heterozygous crosses (80/277; 29%) was close to the expected Mendelian frequency, indicating that homozygous embryos were viable up to parturition (Fig. 2C).

To demonstrate that the ET_A targeted allele is functionally null, we used fibroblasts derived from heterozygous ($ET_A^{+/-}$) and homozygous ($ET_A^{-/-}$) mutant E18.5 embryos in a competitive radioligand binding assay (Fig. 2D). In $ET_A^{+/-}$ cells, we detected a large amount of specific ^{125}I-ET-1 binding that was displaceable by an ET_A-selective synthetic ligand (FR139317) but not by an ET_B-selective ligand (IRL1620). The specific binding sensitive to the ET_A antagonist was absent in $ET_A^{-/-}$ cells, demonstrating lack of functional ET_A receptors. A ^{125}I-ET-1 binding assay performed on membrane preparations from whole near-term embryos gave similar results (data not shown).

Respiratory defects in neonates

At birth, $ET_A^{-/-}$ pups showed several striking characteristics that are virtually identical to those observed in mice deficient either for ET-1 (Kurihara et al., 1994) or endothelin converting enzyme-1 (ECE-1; Yanagisawa et al., 1998) (Fig. 3A). Most striking was the poorly formed mandible that sometimes lacked a midline fusion. Mutant pups also had hypoplastic pinnae and a sunken ventral neck. They were cyanotic, had gasping breathing movements, and died within 30 minutes of birth. E18.5 mutant embryos delivered by Caesarean section followed by tracheostomy survived for more than 25 hours, indicating a structural defect in the upper airway as the primary cause of death. By alleviating mechanical asphyxia in P0 $ET_A^{-/-}$ pups, we were also able to investigate the cental ventilatory responses to atmospheric hypoxia and hypercapnia, an important aspect considering the severe impairment of responses previously observed in P0 $ET\text{-}1^{-/-}$ pups (Kuwaki et al., 1996). When P0 wild-type and $ET_A^{-/-}$ pups breathed room air, the respiratory minute volume was not significantly different between the two groups. However, when pups breathed hypoxic gas (1:1 room air:N_2), ventilatory responses were significantly decreased 17.6% in $ET_A^{-/-}$ mice, compared with an increase of 16.6% in wild-type pups. Similarly, when wild-type and mutant pups breathed hypercapnic gas (5% CO_2-95%O_2), mutant pups showed a decreased breathing response of 8.4%, while the wild-type breathing response markedly increased by 64.0%. Since both the ET_A receptor and ET-1 are found in central nervous system areas that participate in respiratory control (Hori et al., 1992), these current results strongly suggest that ET-1/ET_A-mediated signaling is important in the central control of respiration after birth.

Abnormalities in craniofacial morphogenesis

The physical appearance of mutant pups was indicative of defects in cephalic neural crest derivatives. Thus, we further analyzed the development of individual structures derived from the pharyngeal arches. Meckel's cartilage, the first arch cartilage, was present in E14.5 wild-type ($ET_A^{+/+}$) embryos (Fig. 4A), but was absent in $ET_A^{-/-}$ embryos (Fig. 4B). The cartilaginous rudiment of the hyoid bone (derived from Reichert's cartilage, the second arch cartilage) was evident in wild-type and $ET_A^{-/-}$ embryos by E14.5 (Fig. 4A,B), but in

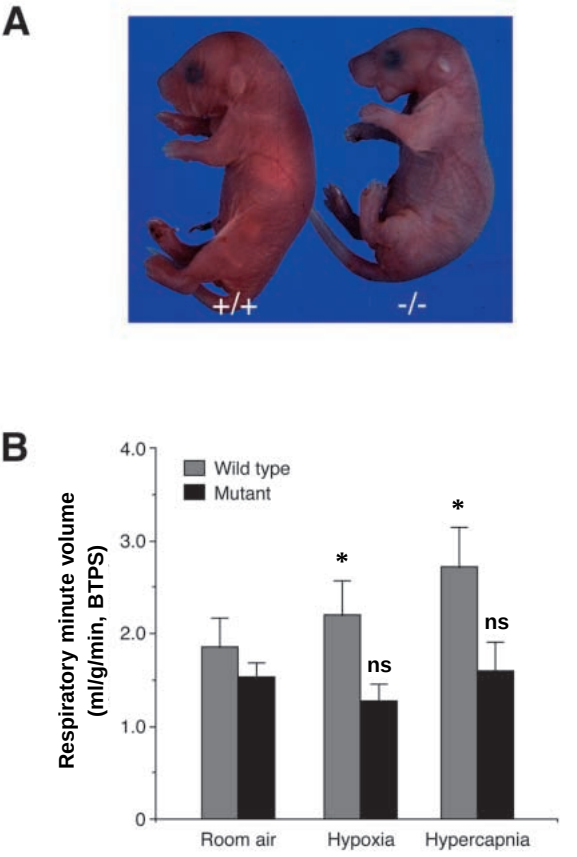

Fig. 3. (A) Gross appearance of P0 $ET_A^{+/+}$ (left) and $ET_A^{-/-}$ (right) pups. Mutant embryos have a shortened mandible, hypoplastic pinnae and appear cyanotic. (B) Respiratory responses of wild-type and homozygous mutant mice delivered by Caesarean section on E18.5. The respiratory minute volume is shown under normal (room air), hypoxic (1:1 room air:N_2), and hypercapnic (5% CO_2-95% O_2) conditions. $ET_A^{-/-}$ pups show an impaired ability to respond to hypoxic and hypercapnic conditions. Values are ± standard error; *P<0.01 from room air (paired t-test); n.s., not significant vs room air. BTPS, normal body temperature, ambient pressure and saturated gas.

the latter it was moved ventrorostrally and fused to a cartilaginous precursor of a cranial bone, forming a ring-like structure. Analysis of E18.5 embryos revealed that this fusion occurred between the lesser horns of the hyoid bone and an area encompassing the basisphenoid bone, the pterygoid bones and the ala temporalis cartilage (Fig. 4D,F). The mandibular bone was hypoplastic, highly disorganized and abnormally articulated with the jugal bone of the zygomatic arch, which itself was smaller than normal (Fig. 4D). Furthermore, aberrant membranous bone extended ventrocaudally from the mandible, forming a disorganized sheet-like structure that fused to endochondral bone near the anterior edge of the basisphenoid bone (Fig. 4D). These fusions resulted in a severe constriction of the upper airway (Fig. 4F), likely contributing to the observed mechanical asphyxia. These abnormalities were exaggerated by the fusion of the soft palate to the lateral floor of the oral cavity proximal to the squamous/respiratory epithelial boundary, and by a thickening of the palate, essentially preventing oral respiration (Fig. 4H). Further, the tongue and associated muscles were

severely hypoplastic (Fig. 4J), the alisphenoid, palatine, ptyergoid and squamosal bones underdeveloped, many of the mandibular salivary and submandibular glands absent, and the thymus hypoplastic and rostrally displaced (data not shown). The penetrance of each of these defects was 100% (14/14 embryos examined). Thus, multiple structures derived from the neural crest component of the first three pharyngeal arches were disrupted in $ET_A^{-/-}$ embryos.

Aberrant middle ear development

Abnormalities of neural crest-derived structures in the middle ear were also observed in 100% (14/14) of $ET_A^{-/-}$ embryos examined. The malleus and incus, as well as the tympanic ring and the cartilaginous anlage of the styloid process, were absent (Fig. 5B), although vestiges of these structures were observed in histological sections (Fig. 5D). This suggests that the rudimentary structures that do form lack normal articulations and are subsequently lost during skeleton staining. The gonial bone was also absent and the cartilaginous rudiment of the third ossicle, the stapes, was absent in 79% (11/14) of mutant embryos (Fig. 5B). The tubotympanic recess, formed by the elongation of the endodermal lining of the first pharyngeal pouch, and the external auditory meatus, formed by the ingrowth of epithelial ectodermal cells, were also absent, and consequentially, so too was the tympanic membrane (Fig. 5D). In situ hybridization analysis clearly shows expression of *ET-1* in the pharyngeal pouches at E9.5 (see Fig. 1D,F), suggesting that loss of the tubotympanic recess is a direct result of loss of ET_A signaling. However, *ET-1* expression is not observed in the epithelial layers around the future external auditory meatus. Its loss is more likely a result of the loss of the tympanic ring, since the tympanic ring primordium is believed to induce early epithelial invagination (Mallo and Gridley, 1996). The inner ear of E18.5 homozygous mutants appeared normal (data not shown).

Defects in distal branches of the trigeminal and facial nerves

Cephalic neural crest cells also contribute to the development of the peripheral nervous system of the head, including the trigeminal, facial and glossopharyngeal ganglia and associated nerves (Le Douarin, 1982). As shown in Fig. 1A, abundant ET_A message is associated with the facial/acoustic neural crest complex at E9.5. This indicates that ET_A signaling may also be important in neuronal development. To investigate this possibility, we performed whole-mount immunohistochemical analysis of neurofilament expression in E10.5 and E11.5 embryos using an anti-NF160 antibody. Examination at low magnification revealed no changes in the peripheral nervous system of $ET_A^{-/-}$ embryos outside the pharyngeal arches. Further, at both ages, the spatial configuration of the

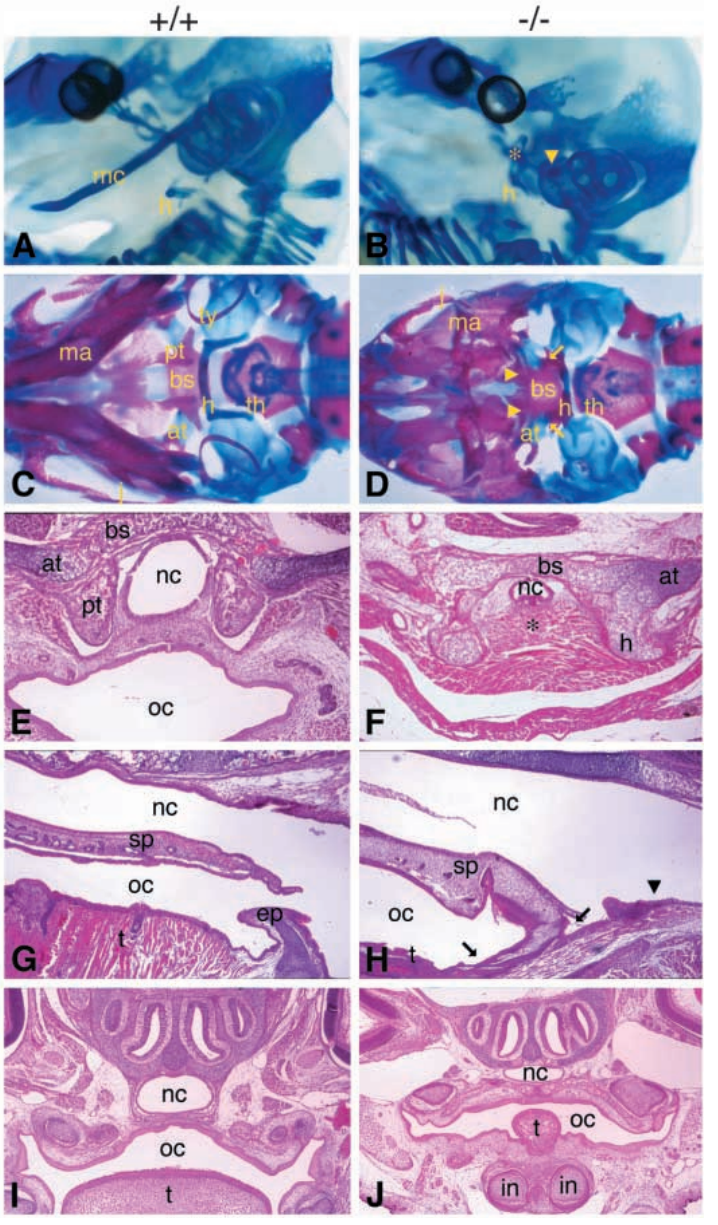

Fig. 4. Analysis of craniofacial defects in $ET_A^{-/-}$ mice. (A-D) Skeleton preparations of $ET_A^{+/+}$ (A, C) and $ET_A^{-/-}$ (B, D) embryos. (A, B) Lateral view of E14.5 littermate skulls (alcian blue). In the mutant, Meckel's cartilage (mc) is absent. The arrowhead points to an abnormal cartilaginous body and the asterisk marks the site of fusion between the cartilaginous precursor of the hyoid (h) bone and the cartilaginous anlage of one or more bones at the base of the skull. (C, D) Ventral view of E18.5 embryo skulls from littermates (alizarin red and alcian blue). The mandible (ma) of the mutant is severely hypoplastic and malformed, the tympanic rings (ty) are absent, and the jugal (j) bone is smaller. A shelf of membranous bone (arrowheads) is also observed extending back from the mandible to the basisphenoid (bs). The fusion points of the hyoid (arrows) appear to encompass the basisphenoid and pterygoid (pt) bones and the ala temporalis (at) cartilage. (E-J) $ET_A^{+/+}$ (E, G) and $ET_A^{-/-}$ (F, H) embryos sectioned in frontal (E, F and I, J) and sagittal (G, H) planes (hematoxylin and eosin). (E, F) Sections at the plane of the basisphenoid bone illustrate the absence of an oral cavity (oc) in the mutant (*). Further, the fusion of the hyoid to the basisphenoid / ala temporalis region is obvious. (G-H) Sections through the midline of the throat show the fusion of the soft palate (sp) in the pharynx (arrows), just proximal to the squamous / respiratory epithelial boundary (arrowhead). Note the proliferation of the soft palate in the mutant. (I, J) The disorganized muscle structure and hypoplasia of the tongue (t) is evident on sections through the mid-tongue region. ep, epiglottis; in, incisor; nc, nasal cavity; th, thyroid cartilage.

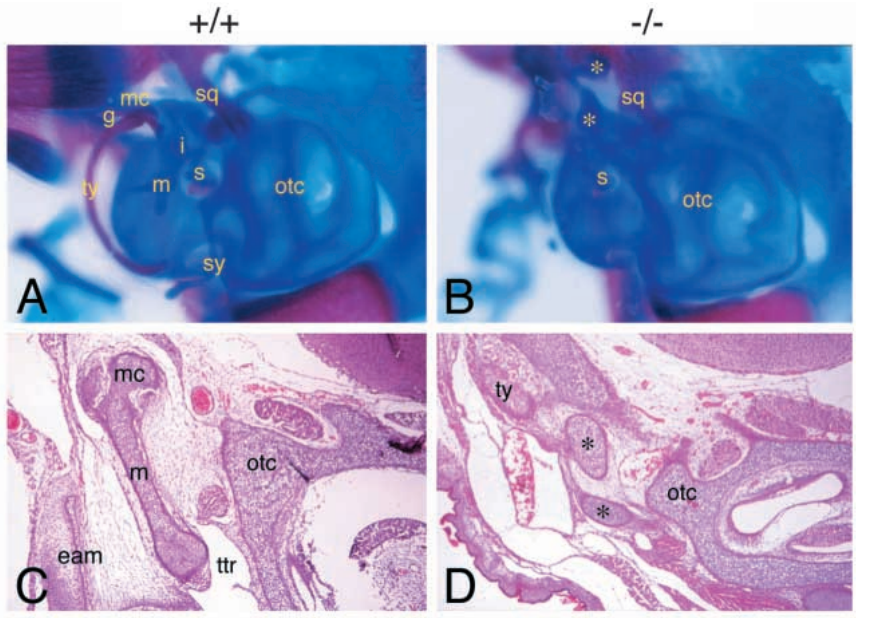

Fig. 5. Middle ear defects in $ET_A^{-/-}$ embryos. (A, B) Skeleton preparations of E18.5 $ET_A^{+/+}$ (A) and $ET_A^{-/-}$ (B) littermates (alizarin red and alcian blue). Lateral view of skull. Note the absence of the tympanic and gonial (g) bones, Meckel's cartilage, malleus (m), incus (i), and styloid process (sy). Two aberrant cartilaginous bodies are marked (*). (C, D) Frontal sections of $ET_A^{+/+}$ (C) and $ET_A^{-/-}$ (D) embryos (hematoxylin and eosin). In mutant embryos, the external auditory meatus (eam) and tubotympanic recess (ttr) are absent, as is Meckel's cartilage and the malleus. Aberrant cartilaginous bodies are marked (*). A rudimentary tympanic ring is observed in the mutant embryo section, but is misplaced and lacks normal articulations. otc, otic capsule; s, stapes; sq, squamosal.

trigeminal, facial and glossopharyngeal ganglia of $ET_A^{-/-}$ embryos appeared normal (Fig. 6B,D). However, while the mandibular branch of the trigeminal nerve and the facial nerve correctly innervated the mandibular and second arches, respectively, the nerves failed to project to the most distal aspects of the $ET_A^{-/-}$arches (Fig. 6B,D). Further, ectopic fiber growth was observed on both the mandibular branch of the trigeminal nerve (Fig. 6D) and the facial nerve (data not shown), whereas the maxillary branch of the trigeminal nerve, which innervates the maxillary portion of the first arch, showed decreased arborization within the frontonasal region (Fig. 6D). These results show that absence of ET_A signaling does not affect the patterning of cranial ganglia, although the distal ends of several nerves emanating from these ganglia are abnormal.

Abnormal cardiac and outflow tract development

There were also numerous abnormalities in the heart and outflow tract of E18.5 $ET_A^{-/-}$ embryos, with a cumulative penetrance of 100%. A common defect observed in the outflow tract was interruption of the aorta (44% occurrence; 7/16 P0 $ET_A^{-/-}$ pups examined suffered this defect), which resulted in a dominant ductus arteriosus that subsequently joined the dorsal aorta (Fig. 7B). Also observed in $ET_A^{-/-}$ embryos were tubular hypoplasia (56%; 9/16), absent right subclavian artery (44%; 4/9), extra arteries branching off the right and left common carotid arteries (23%; 2/9), and right dorsal aorta with right-sided ductus arteriosus (11%; 1/9) (Fig. 7B). A subpopulation of neural crest cells in pharyngeal arches 3, 4 and 6 migrate to the cardiac outflow tract and conotruncal regions, where they are involved in maturation of the great

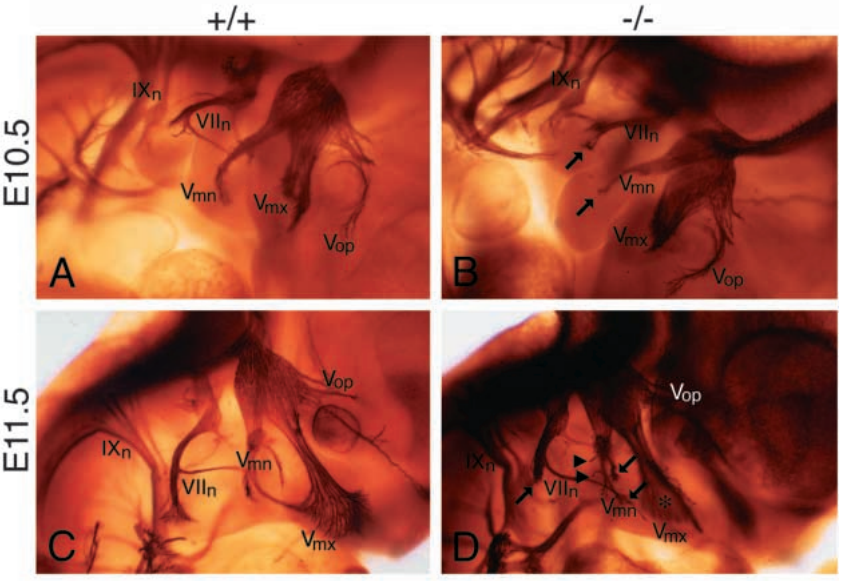

Fig. 6. Peripheral nervous system defects in $ET_A^{-/-}$ embryos. (A-D) Analysis of ganglia and nerve development in E10.5 (A, B) and E11.5 (C, D) $ET_A^{+/+}$ (A, C) and $ET_A^{-/-}$ (B, D) embryos by immunohistochemistry using an anti-NF160 antibody. Lateral view of embryos. (A, B) In E10.5 $ET_A^{-/-}$ embryos, distal projection of the mandibular branch of the trigeminal nerve (V_{mn}) as well as the facial nerve (VII_n) appears abnormal (arrows). (C, D) In E11.5 $ET_A^{-/-}$ embryos, this retardation is more severe (arrows), and ectopic fiber growth is observed on the mandibular branch of the trigeminal nerve (arrowheads). The decreased abortization of the maxillary branch of the trigeminal nerve (V_{mx}) is also indicated (*). V_{op}, ophthalmic branch of the trigeminal nerve; IX_n, glossopharyngeal nerve.

arteries and outflow septation complex (Kirby and Waldo, 1995). Our observation that fourth arch artery derivatives (i.e. a segment of the aortic arch between the left common carotid artery and the left subclavian artery, as well as the proximal right subclavian artery) are most profoundly affected in $ET_A^{-/-}$ (this study) and *ECE-1*$^{-/-}$ mice (Yanagisawa et al., 1998) suggests that cardiac neural crest cells cannot correctly pattern the aortic arch vessels without ET_A receptor-mediated signaling.

We also observed septation and alignment defects in $ET_A^{-/-}$ embryos. Ventricular septal defect (VSD) was observed in 92% (23/25) of E18.5 homozygous mutant embryos (Fig. 7D). The aorta also frequently overrode the defective septum (44%; 11/25). Double outlet-right ventricle (DORV) (28%; 7/25), persistent truncus arteriosus (PTA) (6%; 1/16) and complete transposition of the great arteries (TGA) (13%; 2/16) (Fig. 7D) were also detected. Similar defects have been reported in *ET-1*$^{-/-}$ embryos, but only following administration of anti-ET-1 neutralizing antibodies or ET_A antagonists to pregnant *ET-1*$^{+/-}$ females (Kurihara et al., 1995), illustrating that the effects observed in the present study are a result of loss of ET-1/ET_A interactions. Previous studies in avian systems showed that ablation of the cardiac neural crest results in a highly similar repertoire of phenotypes (Kirby, 1993), strongly suggesting that ET_A receptor disruption affects either the migration or subsequent proliferation/differentiation of cardiac neural crest cells.

Expression of transcription factors in the pharyngeal arches of $ET_A^{-/-}$ embryos

Disruption of cephalic neural crest derivatives in $ET_A^{-/-}$ embryos suggests that ET_A-mediated signaling plays a crucial role in the inductive processes that accompany head development. The complementary expression patterns of ET_A and ET-1 suggest that these molecules affect neural crest development through local interactions within the pharyngeal arch ectomesenchyme, rather than affecting the migration of neural crest cells. Therefore, we examined the expression of two genes known to be expressed in the pharyngeal arches by postmigratory neural crest cells, *Dlx-1* (Price et al., 1991) and *goosecoid* (Blum et al., 1992). These genes are both expressed in the first and second arches at E10.5, although their spatiotemporal expression patterns (Dolle et al., 1992; Gaunt et al., 1993; Qiu et al., 1997) and knockout phenotypes indicate that they are each involved in the development of unique subsets of cephalic neural crest cell derivatives. *Dlx-1*-null mice have defects in the ala temporalis, with partial penetrance of an abnormal phenotype in the stapes, styloid process, and palatine and pterygoid bones (Qiu et al., 1997). Conversely, *goosecoid*-null embryos show defects in multiple craniofacial structures, including the alisphenoid, pterygoid, palatine, tympanic, maxillary, frontal and mandibular bones (Rivera-Perez et al., 1995; Yamada et al., 1995).

Using whole-mount in situ hybridization analysis, *Dlx-1* expression in E10.5 $ET_A^{+/-}$ embryos was observed over the lateral aspects of the first mandibular arch and second arch, a

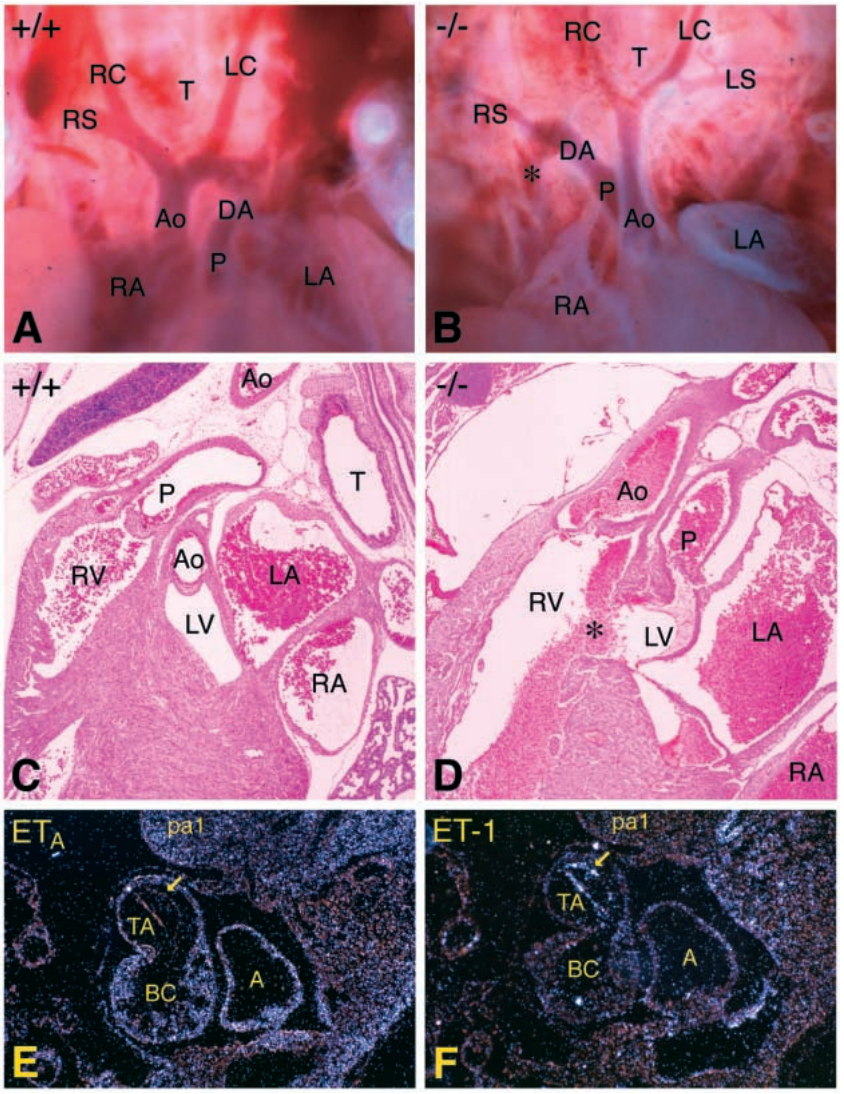

Fig. 7. Cardiac defects in $ET_A^{-/-}$ mice. (A-D) Analysis of E18.5 $ET_A^{+/+}$ (A, C) and $ET_A^{-/-}$ (B, D) embryos. (A, B) Gross examination of the great vessels. In the mutant embryo, the aorta (Ao) gives rise to the right and left common carotid arteries (RC and LC), while the pulmonary outflow (P) forms a dominant ductus arteriosus (DA) and subsequent right-sided dorsal aorta (∗). (C, D) Histological analysis of parasagittal sections through the interventricular septum (hematoxylin and eosin). The perimembranous ventricular septal defect in the mutant is marked (∗). Note the complete transposition of the great arteries (TGA) in the mutant; the aorta arises from the right ventricle (RV), while the pulmonary outflow arises from the left ventricle (LV). (E, F) In situ hybridization analysis of ET_A (E) and *ET-1* (F) transcripts in sagittal heart sections from E9.5 wild-type embryos. ET_A mRNA is observed in the myocardium of the the early heart structures, while *ET-1* mRNA is found in the endocardial layer (arrows). A, atrium; BC, bulbus cordis; RA and LA, right and left atria; RS and LS, right and left subclavian arteries; T, trachea; TA, truncus arteriosus.

pattern that did not change in $ET_A^{-/-}$ embryos. *goosecoid* expression in E10.5 $ET_A^{+/-}$ embryos was observed in the medial aspects of both the posterior half of the first mandibular arch and the anterior half of the second arch, as well as in the nasal pits and limb buds (Fig. 8A). While *goosecoid* expression was not affected in the nasal pits and limb buds of E10.5 $ET_A^{-/-}$ embryos, expression in arches one and two was undetectable. These findings indicate either that expression of *goosecoid* in ectomesenchymal cells requires ET_A-mediated signaling, or that the subpopulation of ectomesenchymal cells that normally express *goosecoid* is absent in $ET_A^{-/-}$ embryos.

DISCUSSION

We inactivated the ET_A gene by targeted deletion of two of the seven transmembrane spanning domains of this G protein-coupled receptor. Homozygous mutant mice exhibit multiple defects in cephalic neural crest cell derivatives. These defects appear to result from loss of inductive signals, both within the pharyngeal arches and their associated arch arteries. Thus, ET_A-mediated signaling appears to define a novel pathway crucial for cephalic neural crest development, and along with the 5-HT2B receptor (Choi et al., 1997), the ET_B receptor (Hosoda et al., 1994), ET-3 (Baynash et al., 1994) and $G\alpha_{13}$ (Offermanns et al., 1997), illustrate the importance of G protein-coupled signaling pathways in embryonic development. Although ET-1 can interact with both ET_A and ET_B receptors with high affinities, the ET-1/ET_A axis does not overlap with the ET-3/ET_B pathway (Baynash et al., 1994; Hosoda et al., 1994), as the enteric neurons of the distal colon and epidermal/choroidal melanocytes were both normal in $ET_A^{-/-}$ mice (data not shown), and defects described in this study were not seen in *ET-3* or ET_B-deficient animals (Baynash et al., 1994; Hosoda et al., 1994).

Epithelio-ectomesenchymal and paraxial mesodermo-ectomesenchymal interactions mediated by the ET-1/ET_A pathway

We have shown in this study that the spatial expression patterns of *ET-1* and ET_A in the pharyngeal arches are complementary to each other and provide a cellular basis for the changes observed in gene expression within the arches of $ET_A^{-/-}$ embryos (Fig. 8B). Reciprocal expression of extracellular ligands and their cognate cell surface receptors often plays a major role in initiating or maintaining morphogenetic changes of developing structures during epithelial/mesenchymal interactions (Andermarcher et al., 1996; Robertson and Mason, 1997). The interaction of ET-1 with the ET_A receptor is likely aided by the spatial distribution of neural crest cells within the arches (Trainor and Tam, 1995). The presence of cephalic neural crest cells just below the surface ectoderm would allow ET-1 expressed by the epithelial cells to act on the ectomesenchymal cells during epithelial/mesenchymal interactions, initiating ET_A signaling. Further regulation of ectomesenchymal development may be imparted by the paraxial mesoderm located in the core of the arch. Neural crest cells and paraxial mesoderm cells are spatially segregated during arch development, possibly allowing paraxial mesoderm to instruct the ectomesenchyme in specific aspects of arch development through interaction of ET-1 with the ET_A receptor. Such action of the mesoderm on the ectomesenchyme may help explain the association of specific arch-derived muscles with skeletal derivatives of the same arch (Kontges and Lumsden, 1996). It is also possible that the

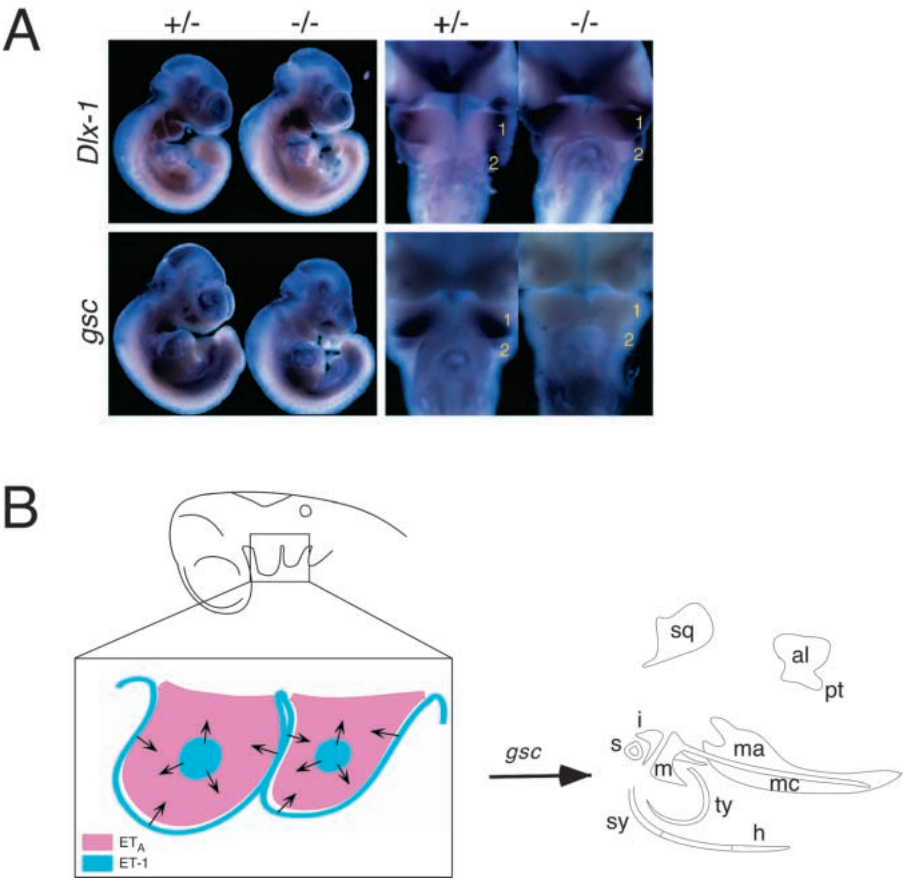

Fig. 8. (A) Whole-mount in situ hybridization of $ET_A^{+/-}$ and $ET_A^{-/-}$ E10.5 embryos using *Dlx-1* and *goosecoid* (*gsc*) riboprobes. Genotype of embryos is indicated, as are pharyngeal arches 1 and 2. While *Dlx-1* and *goosecoid* are both expressed in heterozygous embryos, *goosecoid* expression is absent in homozygous mutant embryos. (B) Proposed model of craniofacial morphogenesis. The interaction of ET-1 (expressed in the epithelium and paraxial mesoderm core of the pharyngeal arches) with the ET_A receptor (expressed by the neural crest-derived ectomesenchymal cells) initiates a signaling cascade that likely includes activation of numerous transcription factors including *goosecoid*. This results in the proper developmental programming of neural crest derivatives in the jaw and neck region. All skeletal elements shown on the right are affected by the ET_A mutation. al, alisphenoid.

ectomesenchyme, having been stimulated by ET-1 from the mesoderm, acts in a reciprocal manner and produces factors that directly influence mesoderm development in a manner similar to the positive feedback loop involving Sonic hedgehog and FGF-4 expression during limb development (Laufer et al., 1994; Niswander et al., 1994). The close proximity of the crest cells with the ectodermal epithelium and paraxial mesoderm is important in this model, as mature ET-1 appears to act over only short distances during development (Yanagisawa et al., 1998).

ET$_A$-mediated signaling and craniofacial development

The *ET$_A$* mutation results in defects in both ectomesenchymal and neuronal derivatives. While the ectomesenchymal defects clearly seems to be a direct result of loss of ET_A signaling, the subtle defects in neurogenic neural crest derivatives could be secondary to other more prominent arch abnormalities, including loss of guidance or growth factors within the pharyngeal arches necessary for distal nerve projection. An elegant scheme of the migration patterns of cephalic neural crest cell subpopulations has been generated through long-term fate mapping (Lumsden et al., 1991; Serbedzija et al., 1992; Couly et al., 1993; Kontges and Lumsden, 1996), and it is possible to use these maps to delineate which crest subpopulations are affected in mice containing targeted gene disruptions (Kontges and Lumsden, 1996). The defects observed in *ET$_A^{-/-}$* embryos indicate that the mutation disrupts the development of cells arising from the posterior midbrain as well as rhombomeres 1, 2, 4 and 6. This suggests that ET_A signaling is required for either initial neural crest migration or in the subsequent maintenance/differentiation of the ectomesenchymal derivatives. Preliminary in situ hybridization analysis has revealed that initial neural crest cell migration appears unaffected in *ET$_A^{-/-}$* embryos (D.E. Clouthier et al., unpublished). This then indicates that the *ET$_A$* mutation results in absence of a signaling pathway that is crucial during further differentiation/development of neural crest derivatives within the arches, likely during epithelial/ectomesenchymal and paraxial mesodermal/ectomesenchymal interactions (Fig. 7B).

goosecoid is a potential downstream effector of ET_A signaling

An intriguing finding of this study is that *goosecoid* expression is absent within the pharyngeal arches of E10.5 *ET$_A^{-/-}$* embryos. This suggests either that ET_A signaling directly or indirectly induces *goosecoid* expression within the neural crest-derived ectomesenchyme, or that the subset of ectomesenchymal cells that normally express *goosecoid* are absent in *ET$_A^{-/-}$* embryos. Based on the expression patterns of several other neural crest markers (D.E. Clouthier et al., unpublished), we believe that the former explanation is more plausible, making *goosecoid* a probable downstream factor in an ET_A receptor signaling pathway. Targeted disruption of *goosecoid* in mice affects similar cell populations to those in *ET$_A^{-/-}$* embryos, although the phenotype is less severe (Rivera-Perez et al., 1995; Yamada et al., 1995). This suggests that *goosecoid* is not the only downstream factor that is disrupted in *ET$_A$* mutant embryos. On the other hand, while *Dlx-1* expression is not affected in *ET$_A$*-deficient embryos, both *ET$_A$*-null and *Dlx-1*-null mice share defects in several skull elements. Thus, *Dlx-1* expression may affect similar downstream targets to ET_A signaling, or function upstream of ET_A receptor signaling.

Lack of ET_A signaling disrupts cardiac neural crest development

While patterning of the outflow tract relies on an extensive bilateral and asymmetrical remodeling of arch arteries (Kirby and Waldo, 1995), the molecular mechanisms that regulate this process are poorly understood (Olson and Srivastava, 1996). This report shows that *ET$_A^{-/-}$* embryos have defects in great vessel alignment and development of the outflow tract. This effect is most certainly ET-1-mediated, as similar phenotypes are observed in *ET-1$^{-/-}$* embryos after treatment of *ET-1$^{+/-}$* pregnant females with neutralizing antibodies against ET-1 or antagonists of the ET_A receptor (Kurihara et al., 1995). Moreover, *ECE-1$^{-/-}$* embryos, in which the levels of mature ET-1 are reduced (Yanagisawa et al., 1998), exhibit virtually identical cardiac defects. These findings are consistent with disruption of cardiac neural crest development, either during migration of the neural crest cells or their subsequent transition from ectomesenchymal cells into the smooth muscle and connective tissues of the arch arteries and septum (Kirby, 1993). Based on the expression patterns of *ET$_A$* and *ET-1* in the developing arch arteries, we suggest that ET-1 expression in the underlying endothelium of the arch arteries provides a microenvironmental signal for the neural crest derived mesenchymal cells of the arch arteries through the ET_A receptor, resulting in the initiation or continuation of arch artery remodeling.

Defects in arch artery development have also been observed following targeted deletion of several others genes in mice, including *RAR* isoforms (Mendelsohn et al., 1994), *NF-1* (Brannan et al., 1994), *NT-3* (Donovan et al., 1996), *Pax3* (Conway et al., 1997) and *dHAND* (Srivastava et al., 1997). Whether any of these genes are involved in the ET_A-mediated signaling pathway is unknown. Interestingly, however, both *dHAND* (Srivastava et al., 1995) and the related gene *eHAND* (Cserjesi et al., 1995) are highly expressed within the pharyngeal arches around E9.5, suggesting that they also play a role in craniofacial development. The fact that *ET$_A$*, *dHAND* and *eHAND* are expressed in two neural crest derived environments during development are further suggestive of a functional relationship.

ET$_A$ and *goosecoid* mutations may cause human craniofacial defects

The phenotype of *ET$_A^{-/-}$* mice resembles a spectrum of human conditions that are collectively termed CATCH 22 (cardiac anomaly, abnormal face, thymic hypoplasia, cleft palate, hypocalcemia, and chromosome 22 deletions) (Wilson et al., 1993) and velocardiofacial syndrome (Shprintzen et al., 1978; Goldberg et al., 1993). Both of these syndromes include numerous cardiac and craniofacial dysmorphisms. While none of the components of the endothelin pathway map to the chromosomal region deleted in CATCH 22 patients (22q11.2), the deletion could affect other components of the same signaling pathway. Indeed, a *goosecoid*-like homeobox gene (*GSCL*) expressed in early human development has recently been mapped within the CATCH 22 minimal critical region (Gottlieb et al., 1997). The phenotypes of *ET$_A^{-/-}$* and *goosecoid$^{-/-}$* mice may help explain how a deletion of a

goosecoid-like molecule leads to pharyngeal arch defects in CATCH 22 patients. Also, microdeletions in chromosome 22 are not ubiquitous among individuals with CATCH 22-like defects, implying the possibility that mutations in *ET_A*, on chromosome 4q28 (our unpublished data), may be responsible for the malformations in a subpopulation of these patients.

We thank Jian Xie, Matthew Wieduwilt, Damiane de Wit, Lucy Lindquist, John Shelton and Robert Webb for technical assistance, Joachim Herz for the JH-1 ES cells, Allan Bradley for the SNL76/7 fibroblast feeder cell line, John L.R. Rubenstein for the *Dlx-1* probe, Richard Behringer and William Shawlot for the *goosecoid* probe and technical help with the whole-mount in situ hybridzations, and Mike Brown and Joe Goldstein for critical reading of the manuscript. M.Y. is an Investigator, and D.E.C. and K.H. are Associates, of the Howard Hughes Medical Institute. This study was supported in part by research grants from the Perot Family Foundation and the W.M. Keck Foundation.

REFERENCES

Andermarcher, E., Surani, M. A. and Gherardi, E. (1996). Co-expression of the *HGF/SF* and c-*met* genes during early mouse embryogenesis precedes reciprocal expression in adjacent tissues during organogenesis. *Dev. Genet.* **18,** 254-266.

Anderson, D. J. (1997). Cellular and molecular biology of neural crest cell lineage determination. *Trends Genet.* **13,** 276-280.

Arai, H., Hori, S., Aramori, I., Ohkubo, H. and Nakanishi, S. (1990). Cloning and expression of a cDNA encoding an endothelin receptor. *Nature* **348,** 730-732.

Baynash, A. G., Hosoda, K., Giaid, A., Richardson, J. A., Emoto, N., Hammer, R. E. and Yanagisawa, M. (1994). Interaction of endothelin-3 with endothelin-B receptor is essential for development of epidermal melanocytes and enteric neurons. *Cell* **79,** 1277-1285.

Benjamin, I., Shelton, J., Garry, D. J. and Richardson, J. A. (1997). Temporospatial expression of the small HSP/αB-crystallin in cardiac and skeletal muscle during mouse development. *Dev. Dyn.* **208,** 75-84.

Blum, M., Gaunt, S. J., Cho, K. W. Y., Steinbeisser, H., Blumberg, B., Bittner, D. and De Robertis, E. M. (1992). Gastrulation in the mouse: the role of the homeobox gene *goosecoid*. *Cell* **69,** 1097-1106.

Brannan, C. I., Perkins, A. S., Vogel, K. S., Ratner, N., Nordlund, M. L., Reid, S. W., Buchberg, A. M., Jenkins, N. A., Parada, L. F. and Copeland, N. G. (1994). Targeted disruption of the neurofibromatosis type-1 gene leads to developmental abnormalities in heart and various neural crest-derived tissues. *Genes Dev.* **8,** 1019-1029.

Bronner-Fraser, M. (1995). Origins and developmental potential of the neural crest. *Exp. Cell Res.* **218,** 405-417.

Chisaka, O. and Capecchi, M. R. (1991). Regionally restricted developmental defects resulting from targeted disruption of the mouse homeobox gene *hox-1.5*. *Nature* **350,** 473-479.

Choi, D.-S., Ward, S. J., Messaddeq, N., Launay, J.-M. and Maroteaux, L. (1997). 5-HT2B receptor-mediated serotonin morphogenetic functions in mouse cranial neural crest and myocardiac cells. *Development* **124,** 1745-1755.

Conway, S. J., Henderson, D. J. and Copp, A. J. (1997). *Pax3* is required for cardiac neural crest migration in the mouse: evidence from the *splotch* (Sp^{2H}) mutant. *Development* **124,** 505-514.

Couly, G. F., Coltey, P. M. and Le Douarin, N. M. (1993). The triple origin of skull in higher vertebrates: a study in quail-chick chimeras. *Development* **117,** 409-429.

Cserjesi, P., Brown, D., Lyons, G. E. and Olson, E. N. (1995). Expression of the novel basic helix-loop-helix gene *eHAND* in neural crest derivatives and extraembryonic membranes during mouse development. *Dev. Biol.* **170,** 664-678.

Davis, C. A., Holmyard, D. P., Millen, K. J. and Joyner, A. L. (1991). Examining pattern formation in mouse, chicken and frog embryos with an *En*-specific antiserum. *Development* **111,** 287-298.

Dolle, P., Price, M. and Duboule, D. (1992). Expression of the murine *Dlx-1* homeobox gene during facial, ocular and limb development. *Differentiation* **49,** 93-99.

Donovan, M. J., Hahn, R., Tessarollo, L. and Hempstead, B. L. (1996). Identification of an essential nonneuronal function of neurotrophin 3 in mammalian cardiac development. *Nature Genet.* **14,** 210-213.

Gaunt, S. J., Blum, M. and De Robertis, E. M. (1993). Expression of the mouse *goosecoid* gene during mid-embryogenesis may mark mesenchymal cell lineages in the developing head, limbs and body wall. *Development* **117,** 769-778.

Goldberg, R., Motzkin, B., Marion, R., Scambler, P. J. and Shprintzen, R. J. (1993). Velo-cardio-facial syndrome: A review of 120 patients. *Am. J. Med. Genet.* **45,** 313-319.

Gottlieb, S., Emanuel, B. S., Driscoll, D. A., Sellinger, B., Wang, Z., Roe, B. and Budarf, M. L. (1997). The DiGeorge syndrome minimal critical region contains a *goosecoid*-like (*GSCL*) homeobox gene that is expressed early in human development. *Am. J. Hum. Genet.* **60,** 1194-1201.

Hori, S., Komatsu, Y., Shigemoto, R., Mizuno, N. and Nakanishi, S. (1992). Distinct tissue distribution and cellular localization of two messenger ribonucleic acids encoding different subtypes of rat endothelin receptors. *Endocrinology* **130,** 1885-1895.

Hosoda, K., Hammer, R. E., Richardson, J. A., Baynash, A. G., Cheung, J. C., Giaid, A. and Yanagisawa, M. (1994). Targeted and natural (piebald-lethal) mutations of endothelin-B receptor gene produce megacolon associated with spotted coat color in mice. *Cell* **79,** 1267-1276.

Hunt, P., Giulisano, M., Cook, M., Sham, M.-H., Faiella, A., Wilkinson, D., Boncinelli, E. and Krumlauf, R. (1991). A distinct *Hox* code for the branchial region of the vertebrate head. *Nature* **353,** 861-864.

Jegalian, B. G. and De Robertis, E. M. (1992). Homeotic transformations in the mouse induced by overexpression of a human *Hox3.3* transgene. *Cell* **71,** 901-910.

Jessel, T. M. and Melton, D. A. (1992). Diffusible factors in vertebrate embryonic induction. *Cell* **68,** 257-270.

Kirby, M. L. (1993). Cellular and molecular contributions of the cardiac neural crest to cardiovascular development. *Trends Cardivasc. Med.* **3,** 18-23.

Kirby, M. L. and Waldo, K. L. (1995). Neural crest and cardiovascular patterning. *Circ. Res.* **77,** 211-215.

Kochhar, D. M. (1973). Limb development in mouse embryos. I. Analysis of teratogenic effects of retinoic acid. *Teratology* **7,** 289-298.

Kontges, G. and Lumsden, A. (1996). Rhombencephalic neural crest segmentation is preserved throughout craniofacial ontogeny. *Development* **122,** 3229-3242.

Kuratani, S. C. and Kirby, M. L. (1991). Initial migration and distribution of the cardiac neural crest in the avian embryo: an introduction to the concept of the circumpharyngeal crest. *Am. J. Anat.* **191,** 215-227.

Kurihara, Y., Kurihara, H., Oda, H., Maemura, K., Nagai, R., Ishikawa, T. and Yazaki, Y. (1995). Aortic arch malformations and ventricular septal defect in mice deficient in endothelin-1. *J. Clin. Invest.* **96,** 293-300.

Kurihara, Y., Kurihara, H., Suzuki, H., Kodama, T., Maemura, K., Nagai, R., Oda, H., Kuwaki, T., Cao, W.-H., Kamada, N., Jishage, K., Ouchi, Y., Azuma, S., Toyoda, Y., Ishikawa, T., Kumada, M. and Yazaki, Y. (1994). Elevated blood pressure and craniofacial abnormalities in mice deficient in endothelin-1. *Nature* **368,** 703-710.

Kuwaki, T., Cao, W.-H., Kurihara, Y., Kurihara, H., Ling, G.-Y., Onodera, M., Ju, K.-H., Yazaki, Y. and Kumada, M. (1996). Impaired ventilatory responses to hypoxia and hypercapnia in mutant mice deficient in endothelin-1. *Am. J. Physiol.* **270,** R1279-R1286.

Laufer, E., Nelson, C. E., Johnson, R. L., Morgan, B. A. and Tabin, C. (1994). *Sonic hedgehog* and *Fgf-4* act through a signaling cascade and feedback loop to integrate growth and patterning of the developing limb bud. *Cell* **79,** 993-1003.

Le Douarin, N. M. (1982). *The Neural Crest.* Cambridge University Press, Cambridge.

Le Douarin, N. M., Ziller, C. and Couly, G. F. (1993). Patterning of neural crest derivatives in the avian embryo: in vivo and in vitro studies. *Dev. Biol.* **159,** 24-49.

Le Lievre, C. S. and Le Douarin, N. (1975). Mesenchymal derivatives of the neural crest: analysis of chimaeric quail and chick embryos. *J. Embryol. Exp. Morphol.* **34,** 125-154.

Lohnes, D., Mark, M., Mendelsohn, C., Dolle, P., Dierich, A., Gorry, P., Gansmuller, A. and Chambon, P. (1994). Function of the retinoic acid receptors (RARs) during development. I. Craniofacial and skeletal abnormalities in RAR double mutants. *Development* **120,** 2723-2748.

Lumsden, A., Sprawson, N. and Graham, A. (1991). Segmental origin and migration of neural crest cells in the hindbrain region of the chick embryo. *Development* **113,** 1281-1291.

Maemura, K., Kurihara, H., Kurihara, Y., Oda, H., Ishikawa, T., Copeland, N. G., Gilbert, D. J., Jenkins, N. A. and Yazaki, Y. (1996). Sequence analysis, chromosomal location, and developmental expression of the mouse preproendothelin-1 gene. *Genomics* **31,** 177-184.

Mallo, M. and Gridley, T. (1996). Development of the mammalian ear: coordinate regulation of formation of the tympanic ring and the external acoustic meatus. *Development* **122,** 173-179.

Martin, J. F., Bradley, A. and Olson, E. N. (1995). The *paired*-like homeo box gene *MHox* is required for early events of skeletogenesis in multiple lineages. *Genes Dev.* **9,** 1237-1249.

Matsuo, I., Kuratani, S., Kimura, C., Takeda, N. and Aizawa, S. (1995). Mouse *Otx2* functions in the formation and patterning of rostral head. *Genes Dev.* **9,** 2646-2658.

McGuinness, T., Porteus, M. H., Smiga, S., Bulfone, A., Kingsley, C., Qiu, M., Liu, J. K., Long, J. E., Xu, D. and Rubenstein, J. L. R. (1996). Sequence, organization, and transcription of the *Dlx-1* and *Dlx-2* locus. *Genomics* **35,** 473-485.

Mendelsohn, C., Lohnes, D., Decimo, D., Lufkin, T., LeMeur, M., Chambon, P. and Mark, M. (1994). Function of the retinoic acid receptors (RARs) during development. 2. Multiple abnormalities at various stages of organogenesis in RAR double mutants. *Development* **120,** 2749-2771.

Niswander, L., Jeffrey, S., Martin, G. R. and Tickle, C. (1994). A positive feedback loop coordinates growth and patterning in the vertebrate limb. *Nature* **371,** 609-612.

Noden, D. M. (1988). Interactions and fates of avian craniofacial mesenchyme. *Development* **103,** 121-140.

Offermanns, S., Mancino, V., Revel, J.-P. and Simon, M. I. (1997). Vascular system defects and impaired cell chemokinesis as a result of $G\alpha_{13}$ deficiency. *Science* **275,** 533-536.

Oh, S. P. and Li, E. (1997). The signaling pathway mediated by the typeIIB activin receptor controls axial patterning and lateral asymmetry in the mouse. *Genes Dev.* **11,** 1812-1826.

Olson, E. N. and Srivastava, D. (1996). Molecular pathways controlling heart development. *Science* **272,** 671-676.

Price, M., Lemaistre, M., Pischetola, M., Di Lauro, R. and Duboule, D. (1991). A mouse gene related to *Distal-less* show a restricted expression in the developing forebrain. *Nature* **351,** 748-751.

Qiu, M., Bulfone, A., Ghattas, I., Meneses, J. J., Christensen, L., Sharpe, P. T., Presley, R., Pedersen, R. A. and Rubenstein, J. L. R. (1997). Role of the Dlx homeobox genes in proximodistal patterning of the branchial arches: Mutations of Dlx-1, Dlx-2, and Dlx-1 and -2 alter morphogenesis of proximal skeletal and soft tissue structures derived from the first and second arches. *Dev. Biol.* **185,** 165-184.

Qui, M., Bulfone, A., Martinez, S., Meneses, J. J., Shimamura, K., Pedersen, R. A. and Rubenstein, J. L. R. (1995). Null mutation of *Dlx-2* results in abnormal morphogenesis of proximal first and second branchial arch derivatives and abnormal differentiation in the forebrain. *Genes Dev.* **9,** 2523-2538.

Rivera-Perez, J. A., Mallo, M., Gendron-Maguire, M., Gridley, T. and Behringer, R. R. (1995). *goosecoid* is not an essential component of the mouse gastrula organizer but is required for craniofacial and rib development. *Development* **121,** 3005-3012.

Robertson, K. and Mason, I. (1997). The GDNF-RET signalling partnership. *Trends Genet.* **13,** 1-42.

Sakurai, T., Yanagisawa, M., Takuwa, Y., Miyazaki, H., Kimura, S., Goto, K. and Masaki, T. (1990). Cloning of a cDNA encoding a non-isopeptide-selective subtype of the endothelin receptor. *Nature* **348,** 732-735.

Satokata, I. and Maas, R. (1994). *Msx1* deficient mice exhibit cleft palate and abnormalities of craniofacial and tooth development. *Nature Genet.* **6,** 348-356.

Schorle, H., Meier, P., Buchert, M., Jaenisch, R. and Mitchell, P. J. (1996). Transcription factor AP-2 essential for cranial closure and craniofacial development. *Nature* **381,** 235-238.

Serbedzija, G. N., Bronner-Fraser, M. and Fraser, S. E. (1992). Vital dye analysis of cranial neural crest cell migration in the mouse embryo. *Development* **116,** 297-307.

Shah, N. M., Groves, A. K. and Anderson, D. J. (1996). Alternative neural crest cell fates are instructively promoted by TGFβ superfamily members. *Cell* **85,** 331-343.

Shawlot, W. and Behringer, R. R. (1995). Requirement for *Lim1* in head-organizer function. *Nature* **374,** 425-430.

Shprintzen, R. J., Goldberg, R. B., Lewin, M. L., Sidoti, E. J., Berkman, M. D., Argamaso, R. V. and Young, D. (1978). A new syndrome involving cleft palate, cardiac anomalies, typical facies, and learning disabilities: Velo-cardio-facial syndrome. *Cleft Palate J.* **15,** 56-62.

Srivastava, D., Cserjesi, P. and Olson, E. N. (1995). A subclass of bHLH proteins required for cardiac morphogenesis. *Science* **270,** 1995-1999.

Srivastava, D., Thomas, T., Lin, Q., Kirby, M. L., Brown, D. and Olson, E. N. (1997). Regulation of cardiac mesodermal and neural crest development by the bHLH transcription factor, dHAND. *Nature Genet.* **16,** 154-160.

Trainor, P. A. and Tam, P. P. L. (1995). Cranial paraxial mesoderm and neural crest cells of the mouse embryo: co-distribution in the craniofacial mesenchyme but distinct segregation in branchial arches. *Development* **121,** 2569-2582.

Trainor, P. A., Tan, S.-S. and Tam, P. P. L. (1994). Cranial paraxial mesoderm: regionalisation of cell fate and impact on craniofacial development in mouse embryos. *Development* **120,** 2397-2408.

Wilkinson, D. G. (1992). Whole mount in situ hybridization of vertebrate embryos. In *In situ Hybridization* (ed. D. G. Wilkinson), pp. 75-83. IRL, Oxford.

Wilson, D. I., Burn, J., Scambler, P. and Goodship, J. (1993). DiGeorge syndrome: Part of CATCH 22. *J. Med. Genet.* **30,** 852-856.

Yamada, G., Mansouri, A., Torres, M., Stuart, E. T., Blum, M., Schultz, M., De Robertis, E. M. and Gruss, P. (1995). Targeted mutation of the murine *goosecoid* gene results in craniofacial defects and neonatal death. *Development* **121,** 2917-2922.

Yanagisawa, M. (1994). The endothelin system: a new target for therapeutic intervention. *Circulation* **89,** 1320-1322.

Yanagisawa, H., Yanagisawa, M., Kapur, R. P., Richardson, J. A., Williams, S. C., Clothier, D. E., de Wit, D., Emoto, N. and Hammer, R. E. (1998). Dual genetic pathways of endothelin-mediated intercellular signaling revealed by targeted disruption of endothelin converting enzyme-1 gene. *Development* **125**, 825-836.

Zhang, J., Hagopian-Donaldson, S., Serbedzija, G., Elsemore, J., Plehn-Dujowich, D., McMahon, A. P., Flavell, R. A. and Williams, T. (1996). Neural tube, skeletal and body wall defects in mice lacking transcription factor AP-2. *Nature* **381,** 238-241.

Zhao, Q., Behringer, R. R. and de Crombrugghe, B. (1996). Prenatal folic acid treatment suppresses acrania and meroanencephaly in mice mutant for the *Cart1* homeobox gene. *Nature Genet.* **13,** 275-283.